Research Article

Molecular Cancer Therapeutics

# Sunitinib Malate and Figitumumab in Solitary Fibrous Tumor: Patterns and Molecular Bases of Tumor Response

Silvia Stacchiotti[1], Tiziana Negri[2], Elena Palassini[1], Elena Conca[2], Alessandro Gronchi[3], Carlo Morosi[4], Antonella Messina[4], Ugo Pastorino[3], Marco A. Pierotti[5], Paolo G. Casali[1], and Silvana Pilotti[2]

## Abstract

Antiangiogenic treatment activity has been reported in solitary fibrous tumor (SFT), a rare and little chemosensitive sarcoma. We explored the activity of sunitinib malate (SM) in SFT and studied receptor tyrosine kinase (RTK) activation profile. Eleven patients with progressive metastatic SFT resistant to chemotherapy were treated with continuous-dosing 37.5 mg/d SM on a named-use basis. One of them also received the insulin-like growth factor I receptor (IGFIR) inhibitor figitumumab after developing secondary resistance to SM. Besides, biochemical, molecular, and fluorescence *in situ* hybridization analyses were done in eight naïve SFTs whose cryopreserved material was available to clarify RTK upstream and downstream signaling. In two cases treated with SM and belonging to the naïve series, both pretreatment and posttreatment samples were available. Ten patients were evaluable for response to SM. The best response according to the Choi criteria was six partial response (all with Response Evaluation Criteria in Solid Tumors stable disease), one stable disease, and three progressive disease. Responses lasted >6 months in five patients. The eight naïve samples showed high expression/phosphorylation of PDGFRB, epidermal growth factor receptor, and IGFIR/IR, in the presence of their cognate ligands. Downstream pathways revealed expression/activation of Akt, extracellular signal-regulated kinase 1-2 and, closely related to SFT subtypes, of S6 and 4E-BP1. In two patients, whose pretreatment and posttreatment clinical and molecular status were available, biochemical data confirmed the activity of SM, although they also suggested a possible time-dependent shift of dominant RTK from PDGFRB to IGFIR/insulin receptor. A Response Evaluation Criteria in Solid Tumors partial response to figitumumab corroborated these findings. SM has antitumor activity in SFT, possibly through a PDGFRB-mediated mechanism, but treatments with IGFIR/insulin receptor and possibly epidermal growth factor receptor inhibitors are worth testing. *Mol Cancer Ther; 9(5); 1286–97. ©2010 AACR.*

## Introduction

Solitary fibrous tumor (SFT) is a very rare sarcoma, mostly occurring in middle-aged patients. SFTs can occur at all anatomic sites: pleura, peritoneum, head and neck, extremities, and viscera (1). SFT is included in the last WHO classification of soft tissue and bone tumors, in the chapter of fibroblastic/myofibroblastic tumors, under the heading "Extrapleural SFT and hemangiopericytoma" (2). Besides, SFT can arise from the central nervous system/meninges, in which the distinction between SFT and hemangiopericitoma is still retained, as reported in the central nervous system tumor WHO classification (3). Usually, SFT has a favorable clinical course. In fact, it has a low tendency to recur after complete surgery, as well as a low metastatic potential (10–15%). Indeed, patients with unresectable or metastatic disease cannot be cured and have an ultimate poor prognosis (4). Even if there is no strict correlation between morphology and behavior, SFTs are classified in "typical" and "malignant." In detail, malignant SFT is defined by at least one of the following criteria: mitotic index of >4/10 high-power microscopic fields, necrosis, and moderate nuclear pleomorfism (2). Rarely, SFT can show over-

**Authors' Affiliations:** [1]Adult Sarcoma Medical Oncology Unit, Department of Cancer Medicine, [2]Experimental Molecular Pathology Unit, Department of Pathology, Departments of [3]Surgery and [4]Radiology, [5]Scientific Directorate, Fondazione Istituto Di Ricovero e Cura a Carattere Scientifico Istituto Nazionale Tumori, Milan, Italy

**Note:** Supplementary material for this article is available at Molecular Cancer Therapeutics Online (http://mct.aacrjournals.org/).

S. Stacchiotti, T. Negri, P.G. Casali, and S. Pilotti contributed equally to this work.

Presented at the 45th American Society of Clinical Oncology Annual Meeting, 2009, Orlando.

**Corresponding Author:** Silvia Stacchiotti, Adult Sarcoma Medical Oncology Unit, Department of Cancer Medicine, Fondazione Istituto Di Ricovero e Cura a Carattere Scientifico Istituto Nazionale Tumori, via Venezian 1, 20133 Milan, Italy. Phone: 39-02-2390-2182; Fax: 30-02-2390-2804. E-mail: silvia.stacchiotti@istitutotumori.mi.it

**doi:** 10.1158/1535-7163.MCT-09-1205

growth or abrupt transition from conventional SFT to high-grade sarcoma. In this case, it is labeled as pleomorphic/dedifferentiated (P/D; refs. 5, 6).

Interestingly, association to hypoglycemia, possibly mediated by insulin growth factors, has been described in 4% to 10% of cases (7–10), more often in SFT arising from peritoneum.

SFTs are known to have a low sensitivity to conventional chemotherapy (11–14). Studies aimed at identifying druggable receptor tyrosine kinases (RTK) in SFTs are few and mainly retrospective. They underline the frequent expression of platelet-derived growth factor receptor (PDGFR) family members (PDGFRB, 86.5%; PDGFRA, 97.7%), MET (96.6%; ref. 15), as well as IGF2 (16). Sporadically missense mutations involving PDGFRB were described (i.e., 2 cases of 88 examined; ref. 15). Interestingly, among the 50+ bone and soft tissue tumors, SFT is the one with the most prominent expression of IGF2, in terms of frequency (20 of 25 cases) and magnitude (16). Furthermore, in a series of eight surgical specimens, the constitutive activation of insulin receptor (IR), mainly represented by the IR-A isoform, and its downstream signaling, was shown through immunoprecipitation (IP), Western blotting (WB), and reverse transcription-PCR (RT-PCR; ref. 17).

Considering that insulin-like growth factor I receptor receptor/insulin receptor (IGFIR/IR) signaling influences numerous other growth factors or receptors, among which is vascular endothelial growth factor (VEGF; ref. 18), and taking into account the frequent involvement of PDGFR in SFT, we explored the use of sunitinib malate (SM) in a group of 11 progressive advanced SFTs resistant to cytotoxic chemotherapy. We report here on the retrospective analysis of this series. We also investigated the biochemical-molecular profile of an explorative series of eight SFTs to gain deeper insights into RTK expression/activation and possible activation mechanisms. Based on the molecular results, one patient with secondary resistance to SM was treated with figitumumab, an IGFR1 inhibitor.

## Materials and Methods

### Clinical methods and treatment

Patients treated in this series had a confirmed diagnosis of locally advanced or metastatic, evidently progressing, PDGFRB-positive SFT, pretreated with at least a front-line chemotherapy. The performance status (Eastern Cooperative Oncology Group) had to be ≤3. Adequate bone marrow and organ function were also requested. In all cases, PDGFRB was assessed by immunohistochemistry and PDGFB mRNA was confirmed by RT-PCR on fixed material (19).

Patient's written informed consent to a nonconventional medical treatment, selected in the lack of alternative therapies known to be effective in the disease, was required. The Ethics committee approved the use of the drug in each case. The drugs were provided by the pharmaceutical company on a named-use basis.

***Sunitinib.*** Patients self-administered 37.5 mg SM orally once daily, without planned treatment breaks. Treatment was continued until disease progression or patient decision. SM was withheld for hematologic grade >3 adverse events and for nonhematologic grade >2 adverse event (defined according to the National Cancer Institute Common Toxicity Criteria, version 3.0) and restarted after recovery to grade <2, in case of hematologic, or grade <1, in case of nonhematologic, toxicity. In case of refractory G3 toxicity with evidence of clinical response to treatment, SM dose reduction to 25 mg/d was allowed. Surgery was considered after 3 to 6 months whenever feasible in all cases independent of response. One more case affected by focal progression after 9 months of treatment underwent surgery of the nonresponding lesion.

***Figitumumab.*** Figitumumab was administered after progression on SM, with >28 days off from SM. Figitumumab was given i.v. at the dose of 30 mg/kg every 28 days.

***Evaluation.*** At baseline, all patients were evaluated with a complete history and physical examination, a complete blood count and serum chemistry, and full cardiologic assessment. Adverse events, serum chemical analyses, and blood count were monitored after 2 weeks from treatment start, then monthly. Imaging studies before treatment included a whole-body computed tomography (CT) scan, and a CT scan and/or magnetic resonance imaging (MRI) of sites of disease, with and without contrast; baseline positron emission tomography (PET) scan was performed in all cases. Scanning was repeated approximately after 4 to 6 weeks from treatment start, than every 2 to 3 months. PET was repeated only if positive at baseline.

***Efficacy assessment.*** Response to treatment was assessed through both the Response Evaluation Criteria in Solid Tumor (RECIST; ref. 20) and the Choi criteria, as recently defined for gastrointestinal stromal tumor (GIST; ref. 21) and adapted to MRI (22), and PET response, in case of positive PET at baseline.

In particular, the Choi criteria are based on changes in tumor size and density following contrast administration on CT scan. We applied the Choi criteria to MRI, assuming that changes in contrast enhancement on subtracted contrast-enhanced T1-weighted sequences parallel changes in density on CT, both being markers of tumor vascularization. Therefore, according to the Choi criteria, a radiological partial response (PR) was defined by the presence of a ≥10% decrease in tumor size or a ≥15% decrease in tumor density/contrast enhancement on CT/MRI, whereas progression was defined by new lesions or, in case of ≥10% increase in tumor, greatest maximal diameter, without any criteria for PR by tumor density/contrast enhancement or ≥15% increase in tumor density/contrast enhancement. Finally, PET response was evaluated according to the currently available European

**Table 1.** Patient characteristics and clinical findings

| Patient | SFT subtype | Previous treatment | Sunitinib dosage | Best response (Choi criteria) | | | Best response (RECIST) | Total no. of cycles | Surgery of residual disease | |
|---|---|---|---|---|---|---|---|---|---|---|
| 1 | P/D | Epirubicin + ifosfamide with PD after two cycles | 37.5 | SD | | | SD | 7 | Yes | Treatment stopped for PD, followed by surgery |
| 2 | Malignant | High-dose ifosfamide with PD after two cycles | 37.5 | PR | | ↓HU | SD | 16 | Yes | Treatment stopped for PD Figitumumab ongoing |
| 3 | Malignant | High-dose ifosfamide with PD after three cycles | 37.5/50 | PR | | ↓HU | SD | 18 | | Ongoing |
| 4 | P/D | Epirubicin + ifosfamide with PD after two cycles | 37.5 | PD | | | PD | 1 | | Treatment stopped for PD (death 2 wk later) |
| 5 | Malignant | High-dose ifosfamide with PD after two cycles | 37.5/25 | PR | ↓Size | ↓HU | SD | 3 | | Treatment stopped due to patient's choice (death 1 mo later) |
| 6 | Malignant | High-dose ifosfamide with PD after five cycles | 37.5 | PD | | | SD | 6 | | Treatment stopped for PD, followed by radiation therapy |
| 7 | Malignant | High-dose ifosfamide with PD after two cycles | 37.5 | PR | | ↓HU | SD | 11 | | Ongoing |
| 8 | Malignant | High-dose ifosfamide with PD after two cycles | 37.5 | PR | ↓Size | | SD | 6 | | Ongoing |
| 9 | malignant | High-dose ifosfamide with PD after three cycles | 37.5 | PD | | | SD | 6 | | Treatment stopped for PD, followed by chemotherapy |
| 10 | P/D | No | 37.5 | PR | ↓Size | ↓HU | SD | 6 | | Treatment stopped for PD, followed by chemotherapy |
| 11 | Malignant | Epirubicin + ifosfamide with PD after 2 cycles | 37.5 | Not evaluable | | | Not evaluable | | | Treatment stopped due to skin toxicity |

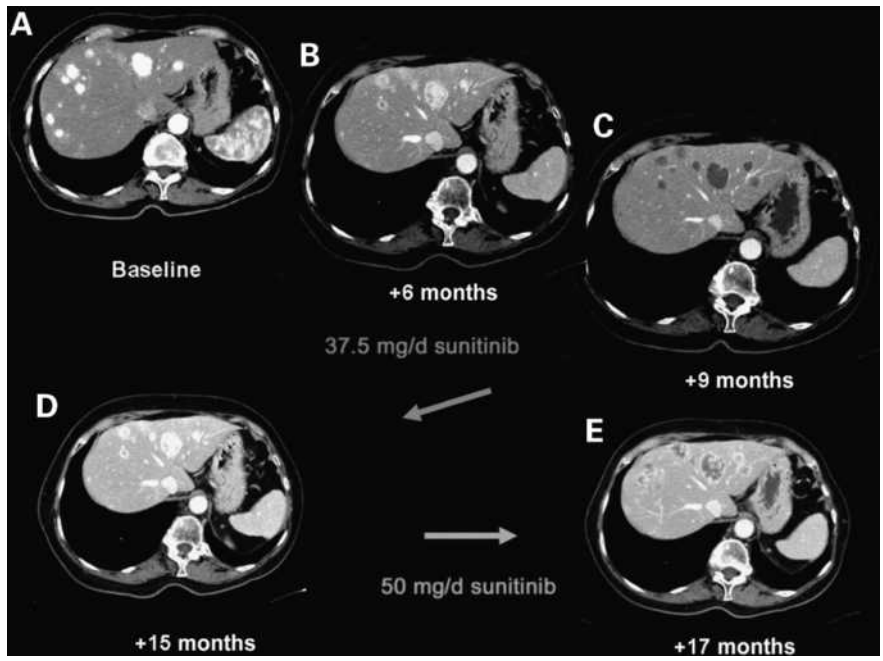


Figure 1. CT scan (arterial phase) showing liver metastasis from peritoneal SFT. A, baseline before starting sunitinib. B, after 3 mo of treatment with 37.5 mg/d sunitinib, evidence of initial decrease in tumor density without changes in tumor size, i.e., Choi PR/RECIST SD. C, the best response to 37.5 mg/d sunitinib achieved after 9 mo of treatment. The lesions are all hypodense, again with no changes in tumor size. D, after 15 mo of treatment with 37.5 mg/d sunitinib, CT scan shows initial signs of progression defined by a diffuse increase in tumor density, without increase in tumor size nor evidence of new lesions. E, new tissue response at 17 mo after increasing the dose of sunitinib to 50 mg/d.

Organization for Research and Treatment of Cancer 1999 tumor response criteria (23).

## Translational methods

***Naïve patients.*** We analyzed a series of eight naïve SFTs (primary/recurrences: 6/2; 1 case metastatic at presentation; typical/malignant/PD: 3/2/3) operated on at our Institution, whose fixed and cryopreserved material was available. All cases were morphologically and immunophenotypically consistent with the diagnosis of SFT according to the WHO classification (CD34+, CD99+, bcl2 variable +; refs. 5, 6).

***Pre-SM– and post-SM–analyzed patients.*** Two patients belonging to this series were treated with SM and underwent posttreatment surgery (Table 1 for patient 1 and 2, undergoing pulmonary metastasectomy and resection of a peritoneal focally progressive lesion, respectively). Fixed and frozen material was obtained, which allowed us to evaluate the tumoral regression/progression and to compare pretreatment and posttreatment biochemical findings, respectively.

*Tissue selection.* The biochemical and molecular analyses were made on representative cryopreserved tissue by checking one H&E-stained frozen section. Fluorescence *in situ* hybridization (FISH) analyses were made using matching formalin-fixed, paraffin-embedded H&E-stained sections that also served to confirm the diagnosis and to evaluate the tumor regression.

*Total protein extraction.* Proteins were extracted from tissue samples stored at −80°C, as previously described (24).

*Phospho-RTK array.* The Proteome Profiler Array kit (ARY001, R&D Systems) was used as previously described (25).

*Immunoprecipitation and Western blotting.* IP/WB analyses of PDGFRB, epidermal growth factor receptor (EGFR), and IGFIR were done as previously reported (25) using equal amounts (1 mg) of protein lysates. In particular for IGFIR IP, 5 μL of anti-IGFIR antibody (#3027L, Cell Signaling Technology) and the HEK-293 cell line (as positive control) were used. To detect the activated receptor, we used anti–phospho-IGFIR/IR antibody (#3024S IGFIR β Tyr1135-1136/IR β Tyr1150-1151, Cell Signaling Technology) and to evaluate its expression anti-IGFIR antibody.

To detect the coimmunoprecipitated proteins, we reincubated the stripped membranes with immunoprecipitated PDGFRB with the antibody for EGFR (sc-03, Santa Cruz Biotechnology; to evaluate PDGFRB/EGFR heterodimers) and the ones with immunoprecipitated IGFIR with antibodies for IR (#3025, Cell Signaling Technology) and EGFR (to investigate the presence of IGFIR/IR hybrids and IGFIR/EGFR heterodimers).

The expression and activation of the downstream targets were detected as previously described (25).

*RNA extraction and real-time PCR to detect RTK ligands.* Total RNA was extracted from fresh frozen tissue and reverse transcribed as previously described (24). Presence or absence of mRNA of EGF and transforming growth factor α (TGFα; EGFR ligands), and IGFI and IGF2 (IGFIR ligands) were analyzed by means of real-time PCR using specific EGF (Hs00153181_M1), TGFα

(Hs00608187_M1), IGFI (Hs01547656_M1), and IGF2 (Hs01005963_M1) probes (Applied Biosystems). The presence of PDGFB (PDGFRB ligand) mRNA was analyzed by RT-PCR as previously described (19).

*DNA extraction and sequencing.* Mutation analyses were made on *PDGFRB, PI3KCA, PTEN, KRAS, NRAS*, and *BRAF* genes, as previously described (26).

*Fluorescence* in situ *hybridization.* FISH analyses were used to investigate the gene status of *PDGFRB* and *IGFIR* as previously reported (26). In particular for *IGFIR* analysis, BAC clone RP11-654A16 labeled with Spectrum Green (Vysis) was used as the FISH probe and CEP15 labeled with Spectrum Orange (Vysis) was used as the control probe.

*Role of the funding source.* Pfizer srl provided both SM and figitumumab, on a case by case basis, and was informed of the results. The corresponding author had the final responsibility for the decision to submit the article for publication and wrote the manuscript in cooperation with all the other authors. The Company played no role in writing or revising the manuscript.

## Results

### Clinical results

***Sunitinib.*** A total of 11 patients (Table 1) with progressive advanced SFT resistant to front-line chemotherapy received SM from July 2008 to September 2009. Ten were evaluable for response, whereas one interrupted his treatment too early (skin toxicity). Among them, three are still on therapy and seven stopped their treatment [six for progressive disease (PD), 1 for his decision]. Pretreatment frozen material obtained within 3 months from starting the treatment was available in two cases.

Mean age 56 years (range, 40–67). The female/male ratio was 7:4 [site: 5 peritoneum, 3 pleura, 1 bladder, 1 ethmoid, 1 meninges; locoregional/metastatic: 5/6, with involvement of the lung (3), liver (3), bone (1), brain (1)]. The WHO Performance Status was less than 2 in 10 cases and three in one case. All patients had been pretreated with one or more surgical procedures (11), radiotherapy (1), and chemotherapy (10) with anthracycline (3) and/or ifosfamide (10). None of them responded to prior chemotherapy. All patients had progressed within 3 months before starting treatment. PET scan at baseline was negative in six cases. Nine patients were evaluated and followed with CT scan and two were followed with MRI.

The median duration of treatment was 6 months (range, 1–19 mo). All patients started with 37.5 mg/d SM, according to a continuous dosing regimen. In two cases, SM was temporarily reduced to 25 mg/d for toxicity. In one case, it was increased to 50 mg/d after secondary progression. Overall, SM was fairly well tolerated. Toxicity was as expected. In one case, G3 skin toxicity was responsible for definitive treatment interruption.

Main nonhematologic toxicities included fatigue (one case, G3), hypothyroidism (one case, G2), diarrhea (one case, G3), nausea and vomiting (one case, G2), and skin toxicity (G3 in one case, resulting in definitive treatment interruption). The most common hematologic toxicities were neutropenia (three patients, no G3–4), chronic

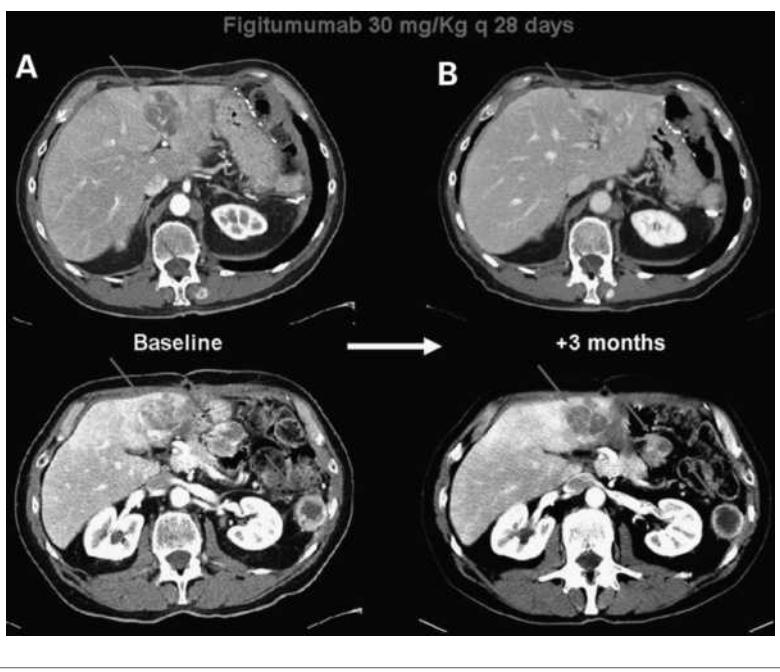


Figure 2. CT scan (arterial phase) showing liver, peritoneal, and soft tissue metastasis from peritoneal SFT. A, baseline before starting figitumumab. B, after 3 mo of treatment with figitumumab, evidence of decrease in tumor size and density, i.e., RECIST PR.

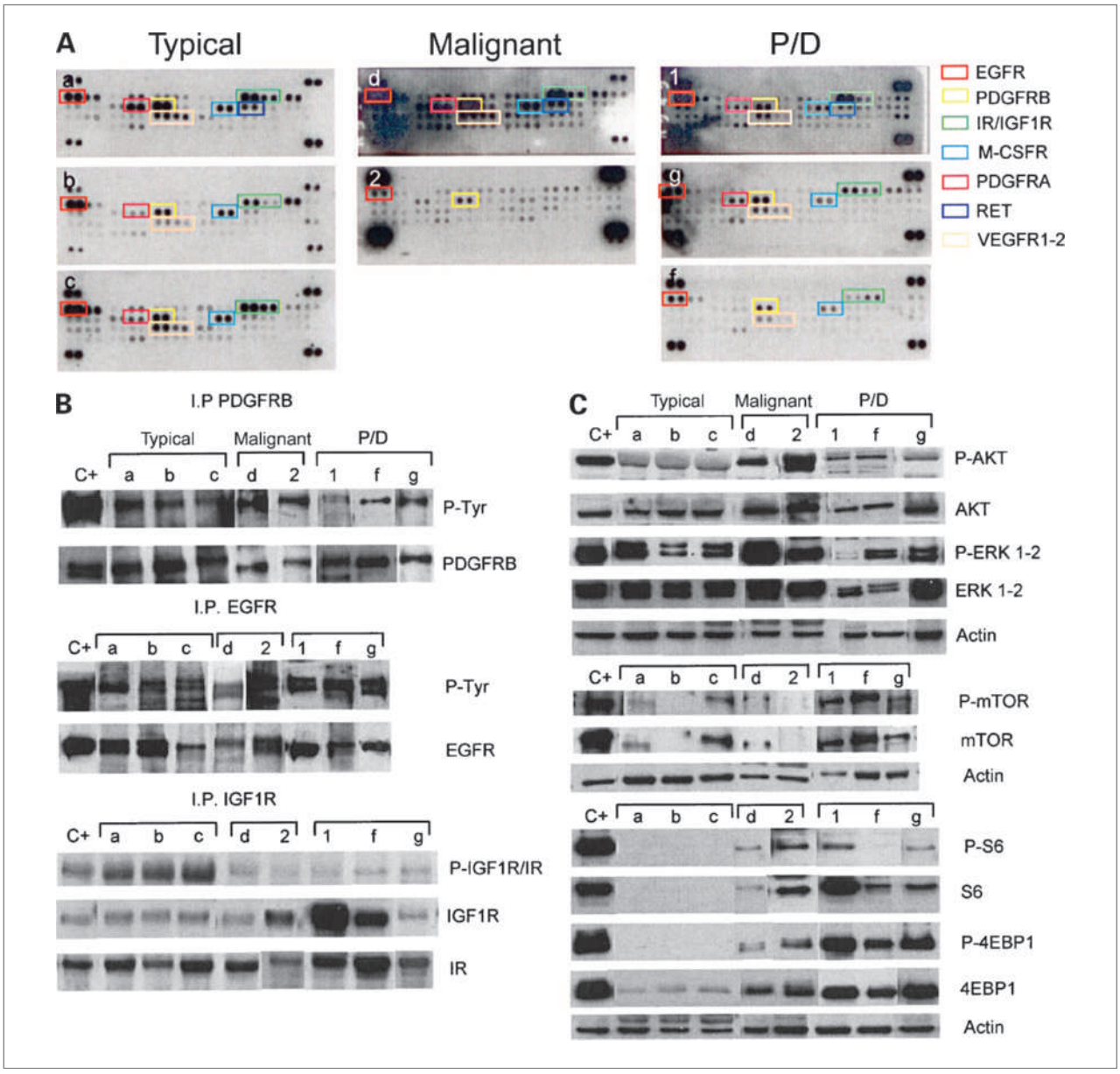


Figure 3. Biochemical analyses of samples from naïve patients. Samples from three typical, two malignant, and three P/D cases were analyzed. A, phospho-RTK arrays. Cases a, b, c, d, f, and g are not described in Table 1; cases 1 and 2 correspond to patients 1 and 2 in Table 1 and to cases depicted in Fig. 4 and 5, respectively. Equal amounts of total protein extracts were incubated with the arrays. The spots (colored rectangles) identify the presence of activated RTKs. B, RTK IP/WB analysis. To confirm the presence of activated PDGFRB, EGFR, and IGFIR/IR, total protein extracts were immunoprecipitated with the specific antibodies and blotted onto a membrane. The PTyr/P-IGFIR/IR panels identify the phosphorylated receptors; PDGFR/EGFR/IGFIR/IR panels indicate the expression of the corresponding receptors. C, downstream signaling analysis. WB experiments showing expression and phosphorylation of AKT, ERK1-2, mTOR, S6, and 4E-BP1. Anti-actin antibody was used to normalize the results.

anemia (one patient, no G3–4), and thrombocytopenia (1 patient, no G3–4).

*Response.* Supplementary Table S1 in the Supplementary Data summarizes clinical findings.

According to RECIST, at 3 months, there were nine stable disease (SD) and one PD, corresponding to six PR (66.6%), one SD (11%), and three PD (33%) as defined by the Choi criteria. A tumor shrinkage took place only in three cases, yet <30%. At 6 months, there were three RECIST PD, corresponding to those patients already progressing according to Choi at 3 months. Choi PR were confirmed at 6 months in all the five patients on treatment for at least 6 months. In all responsive patients, a decrease in tumor density on CT scan or contrast enhancement on MRI was more evident over time (Fig. 1A–C). Posttreatment PET scan, performed only in

two progressive patients, was consistent with the Choi response. One responsive patient stopped his treatment for thyroid-unrelated asthenia and rapidly progressed. He restarted 25 mg/d SM again with response but he asked to discontinue therapy permanently and died 1 month later. Among the two patients on treatment for the longest time, one achieved the best tissue response at 9 months (Fig. 1C). At 15 months, on CT scan, tumor density has started to increase again (Fig. 1D), without evidence of dimensional changes. This was suggestive for initial progression. Interestingly, sides effects decreased during the last 3 months of treatment. So, thinking to a pharmacokinetics basis for progression, we tentatively increased the dose of SM to 50 mg/d, with a new tissue response 2 months later (Fig. 1E).This patient is still on treatment. The second one (patient 2, see below) had a focal progression at 9 months after response and underwent surgery of the progressive lesion. The other radiologically responsive nodules were not resected. After restarting SM, he was without any evidence of further progression 3 months later, but he progressed again after 6 months of treatment. SM was then interrupted. Four weeks later, given the evidence of accelerated progression, figitumumab was initiated (see below). Among the three other progressive patients, one stopped treatment after 1 month and another one stopped treatment after 6 months. The third one (patient 1, see below) had lung lesions from a highly aggressive SFT, albeit apparently progression was slower compared with the pretreatment period, with some lesions unchanged and some increased in size. He stopped SM after 6 months and underwent macroscopically complete lung metastasectomy with evidence of pathologic response in some nodules.

***Figitumumab.*** Patient 2 (male, 68 years), progressing under SM and carrying a suitable IGFIR/IR signaling profile (see below), received figitumumab as from October 2009. He has now received three cycles of treatment and is still on therapy. Treatment was well tolerated without major side effects.

*Response.* PET scan was negative at baseline and was not repeated. Baseline CT scan confirmed PD. It was repeated after one cycle of treatment, 1 day before the second cycle, and showed a dimensional response of all lesions but one. The response was confirmed at 2 months (Fig. 2).

## Translational results

### *Naïve patients*

*Upstream targets*

*Phospho-RTK arrays.* We evaluated the activation profile of RTKs in eight naïve SFTs: three typical, two malignant, and three P/D variant. We observed quite a

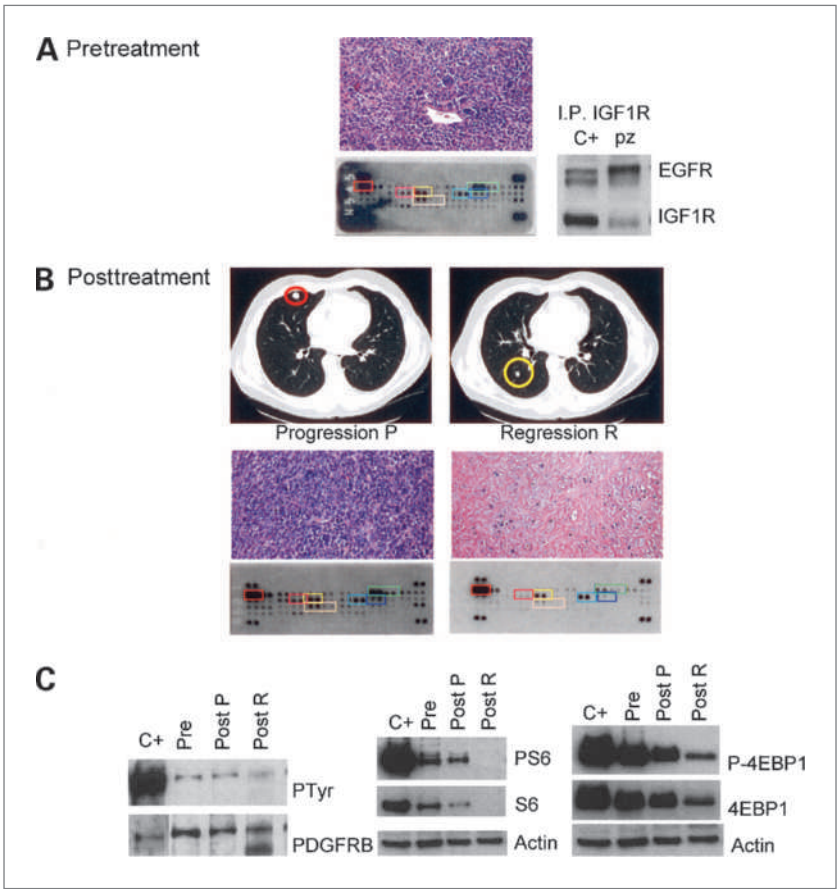


Figure 4. Morphologic and biochemical analyses of pre-SM and post-SM treatment samples of case 1. A, pretreatment findings: P/D SFT, carrying a phospho-RTK array profile characterized by PDGFRB (yellow), EGFR (red), and IGFIR/IR (green) activation. Right, co-IP experiment, using a specific IGFIR antibody, shows EGFR expression together with IGFIR expression. B, posttreatment results: the progressive lesion (P, red circle) is morphologically and biochemically similar to the pretreatment one. On the contrary, the responsive lesion (R, yellow circle) is characterized by cellular depletion coupled with hyaline sclerosis and changing in phospho-RTK array profile with a decreased activation of PDGFRB (yellow), PDGFRA (fuchsia), VEGFR1 (pink) and RET (blue), and IGFIR/IR (green). C, IP/WB: the comparison between pre/posttreatment samples does not show relevant changes in the progressive lesion (P) with respect to PDGFRB, S6, and 4E-BP1 activation, while showing a decrease of phospho-PDGFRB together with the disappearance of S6/P-S6 and a strong decrease of 4E-BP1/P-4E-BP1 in the responsive (R) lesion.

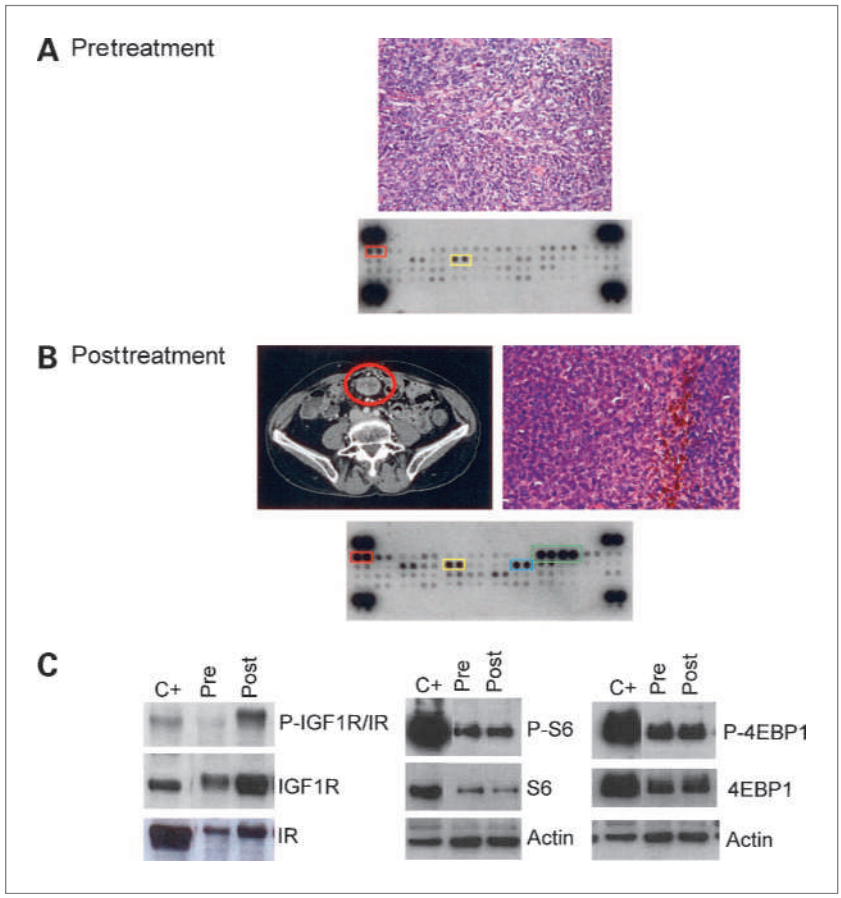


Figure 5. Morphologic-biochemical analyses of pre-SM and post-SM treatment samples of case 2. A, pretreatment findings: high cellular malignant SFT carrying a phospho-RTK array profile characterized by the activation of only EGFR (red) and PDGFRB (yellow). B, posttreatment results: unchanged tumor cellularity with focal evidence of hemosiderin deposits, along with a dramatic change in the activation profile. In particular, there is the evidence of the new occurrence of a highly phosphorylated IGFIR/IR (green) and M-CSFR (blue). The phosphorylation of EGFR and PDGFRB pattern is not changed. C, IP/WB: the comparison between pretreatment and posttreatment blots confirms an increase of IGFIR/IR expression (IGFIR/IR) and phosphorylation (P-IGFIR/IR), whereas S6/P-S6 and 4E-BP1/P-4E-BP1 are still much expressed/phosphorylated.

uniform activation profile, despite the high number of RTK families activated. PDGFRB, EGFR, and IGFIR/IR were the most strongly activated RTKs. Among the SM targets, M-CSFR was moderately activated, whereas PDGFRA, RET, VEGF HER2 receptor 1 (VEGFR1), and VEGFR2 were activated to a lower extent (Fig. 3A). Axl, human HER2/neu, Eph, and RON were found to be poorly activated.

*Immunoprecipitation and Western blotting.* Expression and phosphorylation/activation status of PDGFRB, EGFR, and IGFIR/IR were investigated to confirm the phosphoarray data. They proved to be expressed and activated in all cases (Fig. 3B).

*Coimmunoprecipitation.* Preclinical data suggest that activation was interdependent across receptors, namely that IGFIR forms hybrids with IR (27) and that EGFR may cross-talk with both IGFIR/IR (28) and PDGFRB (29), leading to their transactivation. In particular, IGFIR and IR show a high homology, can form hybrids, and act as bivalent receptors able to bind both insulin and IGFI/IGF2 (27). Accordingly, we performed co-IP experiments. No co-IP was observed between PDGFRB and EGFR, and between PDGFRB and IGFIR (data not shown), whereas in all cases, we showed the presence of IGFIR/IR hybrids (Fig. 3B) and, in case 1, the presence of IGFIR/EGFR heterodimers (Fig. 4A) in addition to another case not shown.

*Analysis of molecular activation mechanism of RTKs.* We investigated the RTK activation by means of autocrine/paracrine loop (ligand mRNA expression), by activating mutations (molecular analysis), and by gene gain (FISH).

*Ligand mRNA expression.* RT-PCR (PDGFB) or real-time PCR (EGF, TGFα, IGFI, and IGF2) showed that all the cases (but one not evaluable) expressed PDGFB (PDGFRB ligand), EGF and TGFα (EGFR ligands), and IGFI and IGF2 (IGFIR, IR, and IGFIR/IR hybrids ligands).

*RTK mutational analysis and FISH analysis. PDGFRB* resulted wild-type and disomic in all cases. No alteration of the *IGFIR* gene profile was observed by FISH analysis.

*Downstream targets*

*Western blotting.* WB experiments were done to investigate the expression/activation status of RTK downstream effectors: AKT and extracellular signal-regulated kinase (ERK)1-2. AKT was expressed with a level of phosphorylation/activation varying from low (typical cases) to strong in all the remaining cases. ERK1-2 were expressed and strongly phosphorylated in all of cases but in case 1. WB was performed to analyze the activation status of mammalian target of rapamycin (mTOR; activated by both AKT and ERK1-2) and its downstream effectors S6 and 4E-BP1. Quite unexpectedly, mTOR was generally expressed and phosphorylated at a low level.

S6 and 4E-BP1 were expressed and phosphorylated in the malignant and P/D SFTs (except for P-S6 in case f), whereas S6 resulted null and 4E-BP1 only expressed a little and not phosphorylated in the typical SFTs. All results are shown in Fig. 3C.

*Mutation analysis. PI3KCA, PTEN, KRAS, NRAS*, and *BRAF* were found to be always wild-type.

***Pretreatment and posttreatment analysis***

*Patient 1*

*Pretreatment sample.* Among the SM targets as described above, PDGFRB was strongly activated in addition to, but to a lower extent, M-CSFR, PDGFRA, RET, and VEGFR1. Moreover, EGFR and IR were strongly activated. EGFR was shown to coimmunoprecipitate with IGFIR (Fig. 4A).

*Posttreatment samples.* We analyzed two metastatic pulmonary nodules corresponding to a radiologically progressive lesion (lesion A in red in Fig. 4B) and to a radiologically stable lesion (lesion B in yellow in Fig. 4B). Lesion A showed morphologic features of progression, whereas lesion B showed features of regression (mainly represented by cellular depletion and increasing of stromal component showing sclerosis and hyalinosis; Fig. 4B). In the progressive sample, RTK activation profile was similar to that observed in the naïve one, whereas in the regressed sample, we detected a decrease of PDGFRB and IR activation, along with a switch-off of PDGFRA, RET, and VEGFR1. The decreased PDGFRB phosphorylation/activation in the regressive sample was confirmed by IP/WB experiments (Fig. 4C). Downstream effectors profile in the regressed lesion parallels the morphologic features. In fact, S6/P-S6 were not present and 4E-BP1/P-4E-BP1 looked much decreased (Fig. 4C).

*Patient 2*

*Pretreatment sample.* The RTK activation was found to be restricted to PDGFRB and EGFR (Fig. 5A).

*Posttreatment sample.* Patient underwent surgery of the radiological progressive lesion, whereas the responsive lesions were not removed. The resected nodule showed morphologic features of progression (Fig. 5B). In this sample, on phospho-RTK-array analysis, PDGFRB and EGFR looked even more activated than before treatment. Furthermore, we observed the *de novo* activation of M-CSFR as well as of IGFIR and IR. The IGFIR/IR phosphorylation/activation increase was confirmed by IP/WB experiments (Fig. 5C). With regards to the downstream pathway, S6/P-S6 and 4E-BP1/P-4E-BP1 resulted expressed and activated as expected in case of progression (Fig. 5C).

## Discussion

We treated 11 patients with progressive, advanced SFT, resistant to first-line chemotherapy, with continuous-dosing SM. Among the 10 patients evaluable for response, at 6 months, six (66.6%) were stable according to RECIST, whereas four progressed. All patients with RECIST SD at 6 months were responsive according to the Choi criteria. One patient with secondary resistance to SM received figitumumab, an IGFIR inhibitor, given molecular evidence of IGFIR activation, and had a dimensional response thereto.

Recently, responses to molecular-targeted and antiangiogenic treatment in SFTs have been reported. In particular, the group of MD Anderson, Houston, reported the activity of bevacizumab in combination with temozolomide (30). The activity of both SM and sorafenib has been reported as well (31–33). SM is a multitargeted RTK inhibitor and antiangiogenic drug with activity against VEGFRs, PDGFRA, PDGFRB, KIT, FLT3, RET, and M-CSFR (34) approved for treatment of GIST and renal cancer (17, 35, 36).

Our data support the activity of SM and preliminary suggest a role for figitumumab in SFT. This is all the more of interest in a tumor known to be poorly sensitive to chemotherapy. Although responses to chemotherapy occasionally may be observed, no patient in this series had responded to cytotoxics. Among patients treated with SM, the best response according to RECIST was a progression arrest. In other words, a "no change" in tumor size was observed (only in one patient was there a decrease of <10%; however, there was also a RECIST SD). This corresponds to what was reported by Dr. S. George and colleagues (31): about three cases of SFT treated with SM and achieving a long-lasting SD, without any RECIST PR. Yet, we also observed that in all patients stable at 6 months, there was a significant change in tumor density and/or contrast enhancement. This change was already present at 3 months and improved at 6 and 9 months. To better quantify this aspect, we decided to apply the Choi criteria as defined for GIST. In GIST, these criteria have been reported to correlate with the outcome much better than RECIST. In fact, even in this series of SFT treated with SM, the Choi criteria looked better than RECIST in identifying tumor response and tumor progression (two patients with RECIST SD at 3 months but without Choi's PR were PD according to RECIST at 6 mo). Interestingly, even in the MD Anderson series of patients treated with bevacizumab in combination with temozolomide, responses were mostly not dimensional, with only one RECIST PR in 11 (79%) responses according to Choi's of 14 treated patients (30). In clinical studies, the alternative is obviously to look at progression-free survival. However, in an exploratory setting as the present one, tumor response is of course more useful. Nonetheless, we also saw an interesting progression-free survival rate at 6 months, indeed quite similar to the one observed in the MD Anderson series. Unfortunately, we could not use PET scan for response assessment because PET was often negative at baseline. As already seen in other solid tumors treated with targeted therapy (i.e., say, GIST, or renal carcinoma treated with sunitinib or with sorafenib; refs. 36, 37), response can take place without dimensional changes. This needs to be considered in further studies on SM in this disease. Tumor response

can last long; among the two patients on treatment, one responded for more than a year. In this case, increasing the dose of SM after progression allowed us to reestablish the response, suggesting that in some cases, progression may be due to pharmacokinetics. Unfortunately, we could not assess drug blood levels. The second patient underwent surgery of the progressive lesion and restarted SM with no evidence of PD 4 months later. In a palliative setting, indeed, limited surgery could add to disease control.

Interestingly, the patient treated with figitumumab had a dimensional tumor response. Figitumumab (CP-751,871) is a fully human IgG2 monoclonal antibody that is specific against the IGFIR (38). It is active in solid tumors, such as lung cancer, as a single agent and in combination with chemotherapy (39). Among sarcomas, IGFIR inhibitors are under study, with evidence of activity in Ewing sarcoma and rhabdomyosarcoma (40). This is the first report on a response to an IGFIR inhibitor in SFT.

The biochemical-molecular analysis of the upstream tyrosine kinase-related pathways in eight naïve SFTs showed the activation of the PDGFR family, as well as EGFR and IGFIR/IR. The RTK activation profile was quite uniform. This supports the notion that such a profile could be distinctive for SFT. In particular, we found an extensive involvement of the PDGFR family (PDGFRB and M-CSFR, and to a lesser extent, PDGFRA) along with RET and VEGFR1/2, which are targeted by SM. We also found the activation of IGFIR/IR in all cases, making the phosphorylation of these receptors family a peculiar trait of SFT, as already reported for IR (17). IGFIR/IR activation was always coupled with activation of EGFR. With respect to downstream signaling, its mechanism of activation seems to be due to an autocrine/paracrine loop, in addition to transactivation between IGFIR and IR (all cases) and IGFIR/EGFR (two cases). In fact, we did not see any upstream and downstream effector deregulation (mutations, gene gains), whereas we saw the expression of the cognate ligands of the activated RTKs. This kind of activation leads to the phosphorylation of a shared downstream signaling (i.e., all RTKs trigger the same signaling), in particular phosphoinositide 3-kinase /AKT and ERK1-2 along with S6 and 4E-BP1, whereas mTOR was expressed and phosphorylated at low level. Interestingly, we found that the P-S6 and P-4E-BP1 level, regardless of the upstream activation, highly mirrors the malignant progression within the gamut of SFT variant (typical, malignant, and P/D). In fact, P-S6 and P-4E-BP1 levels were particularly high in the malignant and P/D variants of SFTs, whereas they were irrelevant in the typical variant, known to show an indolent, although unpredictable, outcome. The data are in line with the concept of the "funnel factor," i.e., with the hypothesis that the activation level of the final effectors more closely parallels the oncogenic role of each individual tumor, irrespective of the upstream oncogenic alterations (41), in particular, the IGFIR/IR make-up that seems to run toward opposite direction. Otherwise, mTOR may represent one of the main phosphorylation pathways of 4E-BP1 and other kinases may be implicated, as shown by our downstream data (Fig. 4C).

The response to SM was confirmed pathologically and biochemically in one of the two patients who underwent surgery (Fig. 4). In fact, lesions that were radiologically stable were pathologically shown to encompass areas of tumor regression, when compared with the pretreatment specimens. Biochemically, in the regressed areas we detected decreased PDGFRB phosphorylation and a switch off of PDGFRA, VEGFR1, and RET, all targets of SM, along with decreased IR phosphorylation. By contrast, in the focal progression shown in Fig. 5, the posttreatment morphology was consistent with a no response. Biochemically, we found M-CSFR (target of SM) activation, in addition to a strong activation of IGFIR/IR, both of which were negative at presentation (this was the only case negative at baseline). This suggests a loss of SM efficacy over time and a possible time-developing shift from one dominant receptor (PDGFRB) to another (IGFIR/IR). Furthermore, in both cases, the progressing posttreatment samples did not show any decrease in EGFR activation. This result might also suggest that EGFR may contribute to disease progression. Consistently, in case 1, we showed a physical interaction, by co-IP, between EGFR and IGFIR. In breast cancer, the same mechanism has been shown to contribute to resistance to anti-EGFR family agents (42). After treatment in both cases, the downstream signaling appeared to be rather activated. This seems to underline the importance of IGFIR/IR-phosphoinositide 3-kinase/AKT/ERK1-2 in SFT and may suggest that SM was active only against a subset of cells, whereas others remained insensitive. Cumulatively, our molecular data provide evidence of the activity of SM both in case of response and in case of primary or secondary resistance. Besides, the response observed to figitumumab, even if very preliminary, sustains the commitment of the IGFIR pathway in SFT and suggests a possible role for IGFIR inhibitor in this disease.

Although our results need confirmation, they support the antitumor activity of SM in SFT. This seems to be largely mediated by PDGFRB with the contribution of IGF1R/IR signaling in particular in resistant cases. Furthermore, IGFIR/IR and EGFR inhibitors seem worth testing, both as single agents and in combination.

## Disclosure of Potential Conflicts of Interest

S. Stacchiotti, E. Palassini, and P.G. Casali received research funds from Pfizer. P.G. Casali received advisory board compensation from Pfizer.

## Acknowledgments

We thank the following pathologists who kindly contributed case material: Agnese Assi (Ospedale Civile, Legnano, Milano), Massimo Brisigotti (Ospedale Infermi, Rimini), Carlo Capella (Ospedale di Circolo e Fondazione Macchi, Varese), Claudio Clemente (Istituto Clinico Sant' Ambrogio, Milano), Guido Monga (Ospedale Maggiore della Carità, Novara), Giorgio Gardini (Arcispedale S. Maria Nuova, Reggio Emilia), Antonio Perna (Ospedale M. Scarlato, Scafati, Salerno),

Massimo Roncalli (Istituto Clinico "Humanitas" Istituto Di Ricovero e Cura a Carattere Scientifico, Rozzano, Milano).

## Grant Support

Italian Ministry of Health (5/1000 Project) grant, and by Associazione Italiana per la Ricerca sul Cancro (Associazione Italiana per la Ricerca sul Cancro).

The costs of publication of this article were defrayed in part by the payment of page charges. This article must therefore be hereby marked *advertisement* in accordance with 18 U.S.C. Section 1734 solely to indicate this fact.

Received 12/29/2009; revised 02/24/2010; accepted 03/24/2010; published 05/10/2010.

## References

1. Chan JKC. Solitary fibrous tumor: everywhere, and a diagnosis in vogue. Histopathology 1997;31:568–76.
2. Tumours of Soft tissue and Bone. Pathology and Genetics. In: Fletcher CDM, Unni KK, Mertens F, editors. World Health Organization Classification of Tumours. Lyon: IARC Press; 2002.
3. WHO classification of tumours of the central nervous system. In: Louis DN, Ohgaki H, Wiestler OD, Cavenee WK, editors. World Health Organization Classification of Tumours. 4th ed Lyon: International Agency for Research on Cancer; 2007.
4. Cranshaw IM, Gikas PD, Fisher C, Thway K, Thomas JM, Hayes AJ. Clinical outcomes of extra-thoracic solitary fibrous tumours. Eur J Surg Oncol 2009;35:994–8.
5. Mosquera JM, Fletcher CDM. Expanding the spectrum of malignant progression solitary fibrous tumor—a study of 8 cases with a discrete anaplastic component—Is this dedifferentiated SFT? Am J Surg Pathol 2009;33:1314–21.
6. Macarenco RS, Erickson-Jhonson MR, Wang X, Folpe AG, Oliveira AM. Dedifferentiated solitary fibrous tumors: a clinicopathologic study of 7 cases. Presented at 45th Annual Meeting of the American Society for Clinical Oncology. Orlando. 2009.
7. Fukasawa Y, Takada A, Tateno M, et al. Solitary fibrous tumor of the pleura causing recurrent hypoglycemia by secretion of insulin-like growth factor II. Pathol Int 1998;48:47–52.
8. Guglielmi A, Frameglia M, Iuzzolino P, et al. Solitary fibrous tumor of the liver with CD 34 positivity and hypoglycemia. J Hepatobiliary Pancreat Surg 1998;5:212–6.
9. Famà F, Le Bouc Y, Barrande G, et al. Solitary fibrous tumour of the liver with IGF-II-related hypoglycaemia. A case report. Langenbecks Arch Surg 2008;393:611–6.
10. Wagner S, Greco F, Hamza A, Hoda RM, Holzhausen HJ, Fornara P. Retroperitoneal malignant solitary fibrous tumor of the small pelvis causing recurrent hypoglycemia by secretion of insulin-like growth factor 2. Eur Urol 2009;55:739–42.
11. Beadle GF, Hillcaot BL. Treatment of advanced malignant hemangiopericytoma with combination adriamycin and DTIC: a report of four cases. J Surg Oncol 1983;22:167–70.
12. Ferigo N, Cottalorda J, Allard D, et al. Successful treatment via chemotherapy and surgical resection of a femoral hemangiopericytoma with pulmonary metastasis. J Pediatr Hematol Oncol 2006;28:237–40.
13. Chamberlain MC, Glantz MJ. Sequential salvage chemotherapy for recurrent intracranial hemangiopericytoma. Neurosurgery 2008;63: 720–6.
14. Shiono S, Abiko M, Tamura G, et al. Malignant solitary fibrous tumor with superior vena cava syndrome. Gen Thorac Cardiovasc Surg 2009;57:321–3.
15. Schirosi L, Lantuejoul S, Cavazza A, et al. Pleuro-pulmonary solitary fibrous tumors: a clinicopathologic, immunohistochemical, and molecular study of 88 cases confirming the prognostic value of de Perrot staging system and p53 expression, and evaluating the role of c-kit, BRAF, PDGFRs (α/β), c-met, and EGFR. Am J Surg Pathol 2008;32:1627–42.
16. Steigen SE, Schaeffer DF, West RB, Nielsen TO. Expression of insulin-like growth factor 2 in mesenchymal neoplasms. Mod Pathol 2009;22:914–21.
17. Li Y, Chang Q, Rubin BP, et al. Insulin receptor activation in solitary fibrous tumours. J Pathol 2007;211:550–4.
18. Tao Y, Pinzi V, Bourhis J, Deutsch E. Mechanisms of disease: signalling of the insulin-like growth factor 1 receptor pathway-therapeutic perspectives in cancer. Nat Clin Pract Oncol 2007;4:591–602.
19. Lagonigro MS, Tamborini E, Negri T, et al. PDGFRα, PDGFRβ and KIT expression/activation in conventional chondrosarcoma. J Pathol 2006;208:615–23.
20. Therasse P, Arbuck SG, Eisenhauer EA, et al, European Organization for Research and Treatment of CancerInstitute of the United States-National Cancer Institute of Canada. New guidelines to evaluate the response to treatment in solid tumors. J Natl Cancer Inst 2000;92: 205–206.
21. Choi H, Charnsangavej C, Faria SC, et al. Correlation of computed tomography and positron emission tomography in patients with metastatic gastrointestinal stromal tumor treated at a single institution with imatinib mesylate: proposal of new computed tomography response criteria. J Clin Oncol 2007;25:1753–9.
22. Stacchiotti S, Collini P, Messina A, et al. Tumor response assessment in high grade soft tissue sarcomas (STS): a pilot study to assess the correlation between radiological and pathological response using both RECIST and Choi's criteria. Radiology 2009; 251:447–56.
23. Young H, Baum R, Cremerius U, et al, European Organization for Research and Treatment of Cancer (EORTC) PET study group. Measurement of clinical and subclinical tumour response using I18FI-fluorodeoxyglucose and positron emission tomography: review and 1999 EORTC recommendations. Eur J Cancer 1999;35: 1773–82.
24. Tamborini E, Bonadiman L, Negri T, et al. Detection of overexpressed and phosphorylated wild-type kit receptor in surgical specimens of small cell lung cancer. Clin Cancer Res 2004;10:8214–9.
25. Tamborini E, Virdis E, Negri T, et al. Analysis of receptor tyrosine kinases (RTK) and downstream pathways in chordomas. Neuro-oncol, In press.
26. Perrone F, Da Riva L, Orsenigo M, et al. PDGFRA, PDGFRB, EGFR, and downstream signalling activation in malignant peripheral nerve sheath tumor. Neuro-oncol 2009;11:725–36.
27. Belfiore A. The role of insulin receptor isoforms and hybrid insulin/IGF-I receptors in human cancer. Curr Pharm Des 2007;13:671–86.
28. Jin Q, Esteva FJ. Cross-talk between the ErbB/HER family and the type I insulin-like growth factor receptor signalling pathway in breast cancer. J Mammary Gland Biol Neoplasia 2008;13:485–98.
29. Liu P, Anderson RGW. Spatial organization of EGF Receptor transmodulation by PDGF. Biochem Biophys Res Commun 1999;261: 695–700.
30. Park MS, Patel SR, Ludwig JA, et al. Combination therapy with temozolomide and bevacizumab in the treatment of hemangiopery-cytoma/malignant solitary fibrous (Abstract). J Clin Oncol 2008; 26:10512.
31. George S, Merriam P, Maki RG, et al. Multicenter phase II trial of sunitinib in the treatment of non-gastrointestinal stromal tumor sarcomas. J Clin Oncol 2009;27:3154–60.
32. Mulamalla K, Truskinovsky AM, Dudek AZ. Rare case of hemangiopericytoma responds to sunitinib. Transl Res 2008;151:129–33.
33. Domont J, Massard C, Lassau N, et al. Hemangiopericytoma and antiangiogenic therapy: clinical benefit of antiangiogenic therapy (sorafenib and sunitinib) in relapsed Malignant Haemangioperyctoma/Solitary Fibrous Tumour. Invest New Drugs 2010; 28:199–202.
34. Chow LQ, Eckhardt SG. Sunitinib: from rational design to clinical efficacy. J Clin Oncol 2007;25:884–96.
35. Demetri GD, van Oosterom AT, Garrett CR, et al. Efficacy and safety of sunitinib in patients with advanced gastrointestinal stromal tumour

after failure of imatinib: a randomised controlled trial. Lancet 2006; 368:1329–38.
36. Motzer RJ, Michaelson MD, Redman BG, et al. Activity of SU11248, a multitargeted inhibitor of vascular endothelial growth factor receptor and platelet-derived growth factor receptor, in patients with metastatic renal cell carcinoma. J Clin Oncol 2006;24:16–24.
37. Ratain MJ, Eisen T, Stadler WM, et al. Phase II placebo-controlled randomized discontinuation trial of sorafenib in patients with metastatic renal cell carcinoma. J Clin Oncol 2006;24:2505–12.
38. Haluska P, Shaw HM, Batzel GN, et al. Phase I dose escalation study of the anti insulin-like growth factor-I receptor monoclonal antibody CP-751,871 in patients with refractory solid tumors. Clin Cancer Res 2007;13:5834–40.
39. Karp DD, Paz-Ares LG, Novello S, et al. Phase II study of the anti-insulin-like growth factor type 1 receptor antibody CP-751,871 in combination with paclitaxel and carboplatin in previously untreated, locally advanced, or metastatic non-small-cell lung cancer. J Clin Oncol 2009;27:2516–22, Epub 2009 Apr 20.
40. Patel S, Pappo A, Crowley J, et al. A SARC global collaborative phase II trial of R1507, a recombinat human monoclonal antibody to the insulin-like growth factor-1 receptor in patients with recurrent or refractory sarcomas. Presented at the 45th Annual Meeting of the American Society for Clinical Oncology. Orlando (FL). 2009.
41. Armengol G, Rojo F, Castellví J, et al. 4E-binding protein 1: a key molecular "funnel factor" in human cancer with clinical implications. Cancer Res 2007;67:7551–5.
42. Nahta R, Yuan LX, Zhang B, Kobayashi R, Esteva FJ. Insulin-like growth factor-I receptor/human epidermal growth factor receptor 2 heterodimerization contributes to trastuzumab resistance of breast cancer cells. Cancer Res 2005;65:11118–28.